

DIRECT CONSTRAINTS ON THE TIMING OF MARTIAN VALLEY NETWORK FORMATION DERIVED USING BUFFERED CRATER COUNTING. C. I. Fassett and J. W. Head III, Dept. of Geological Sciences, Brown University, Providence, RI 02912 (Caleb_Fassett@brown.edu and James_Head@brown.edu).

Introduction: Valley networks on Mars are mostly found in the heavily cratered highland terrain that dates from the Noachian era (the earliest period of martian history) [e.g., 1]. These valley features are commonly invoked as geomorphological evidence for an early surface environment differing from that of today [2], although their implications for climate has continued to be controversial [e.g., 3]. Because the processes of valley network formation are important for understanding surface conditions on early Mars, there has long been substantial interest in constraining when valleys were active [e.g., 4, 5] and when the transition occurred from a "valley network-forming" planet to the Mars we see today.

The global distribution of valley networks and their common presence only on Noachian surfaces has led most workers to the interpretation that valleys are old (earliest Hesperian or Noachian) [1], with a few possible exceptions of valleys on a few volcanoes and on plateau surfaces around Valles Marineris [6,7]. However, others have disagreed with this general view [8], pointing to the fact that some valleys in the highlands appear to cross into units mapped as Hesperian or even Amazonian, and certain valleys appear fresher than others. To address these issues, we have attempted to derive direct constraints on the superposed populations of craters for individual valley systems.

Methodology: Valley Floor Counts: Crater counting typically relies on the assessment of the number of superposed craters on a given mapped unit [e.g., 9, 10]. A major difficulty in directly applying this approach to valley networks is that they have minimal surface areas, which thus requires reliance on small craters for age determination. It is clear that small craters on the floor of valleys are particularly susceptible to removal by mass wasting and aeolian processes. This causes counts on valley floors to typically yield much younger model ages than counts on the surrounding terrains using larger craters. Thus, these counts are unlikely to result in reliable valley network formation ages, even putting aside other uncertainties about small craters production [11].

Counts on Valley-Incised Units: The technique that has been most commonly applied for determining the period of valley network activity is measurement of the crater population of a given terrain transected by valleys. This has the advantage of allowing for crater counting over a much wider area than is incised by a given valley itself, but has the disadvantage that it typically will provide only an upper limit for the activity of a valley. In other words, a valley network found cutting across mid-Noachian terrain is only constrained to be post-mid-Noachian. It also requires the careful delineation of what surface has been incised; inclusion of surroundings with a different age (either significantly younger or older) than the incised unit can lead to incorrect age assignment.

Buffered Crater Counting: We have chosen an alternative approach, counting around valleys in a series of buffers

(Fig. 1), as has been attempted before for other planetary surface features [e.g., 12]. The advantage of this technique is that it utilizes the fact that large craters subtend a much larger area than small ones. We first map the valley we wish to examine, and then find all craters clearly superposed upon the valley which a within an area appropriate for its diameter. For each crater (and its ejecta), a stratigraphic judgment is required, and we assume that any topographic barrier (e.g., a crater rim or its ejecta) that is superposed on a valley and is unmodified by further valley activity must have formed after valley activity ceased. Only craters which are clearly superposed are included, so our results should be a robust minimum (lower) age limit for the last activity in the valley.

For a given crater size D , we count in a buffer of size $1.5D$ from each valley side (Fig. 1). In doing so, we are assuming that it is possible to determine stratigraphic relationships for craters with rims within one crater diameter of the valley walls (consistent with expectations from scaling laws that the extent of continuous ejecta is roughly $\sim 1D$ [13]). As an example, the total count area A that we use for a linear segment of a valley (length L) and a crater of diameter D is $A(D)=(3D+W_v)L$, where W_v is the valley width (Fig. 1). Appropriate count areas are computed for a given crater size by applying the ArcMap buffer function to the mapped valleys (taking into account that buffers for multiple line segments can overlap; where this happens, they are only included once).

Results: Counts have been completed on 30 valley network systems (Table 1), including a variety of regions where valleys are thought likely to be young [6,7,8] and representing a broad sample of the valley systems on the planet (Fig. 2). For each of these systems, we determine the period when the valley was last active and convert the measured size-frequency distributions into absolute ages using both the Neukum [9] and Hartmann [10] production functions (two examples are shown in Fig. 3). We calculate the best-fit ages and errors using a least-squares technique (see Figs. 3, 4). Note that when fitting the cumulative distribution functions (in the Neukum case), we truncate the distributions to exclude craters with $D > 20$ km, to avoid effects of incompleteness at the largest crater sizes (not truncating would lead to an average reduction in $N(5)$ of $\sim 10\%$). Results for the 26 highland valleys, and 4 regions where potentially younger valleys occur, are given below (Table 1, Fig. 4).

Highlands Valleys: Valleys in the Martian highlands commonly are dated to near the Noachian-Hesperian boundary or earlier (Fig. 4). Where valleys appear to cross unit boundaries into regions mapped as Hesperian or even Amazonian [8], we find little evidence that the valleys themselves are younger than the Early Hesperian. Instead, this younger interpretation may have resulted from the difficulty in precisely locating unit boundaries (especially using low-resolution data), as well as the fact that some valleys may have been seen through thin superposed later units.

Our results imply that across the highlands, valley network formation ceased by ~ 3.5 Gyr (Hartmann system [10], see Fig. 4) or ~ 3.7 Gyr (Neukum system [9]). This is consistent with a global shift in surface conditions between the period before and after the Early Hesperian.

Younger Valleys: As has been noted before, a few valley systems have been considered to be prime candidates for valley network activity in more recent periods of martian history [6,7], primarily based on stratigraphic constraints. In four regions, we determined ages for probable young valley network systems, and in each case our counts are in fact considerably younger than the 26 other valley networks dated (Early Amazonian or Late Hesperian). Crater densities on these young systems are lower than typical highland valley networks by a factor of ~ 2 -3 (Table 1, Figs. 3 and 4). In each case, these valley systems are located outside the highlands terrain where most valley networks are found on Mars: three of these examples are found on volcanoes, Ceraunius Tholus, Hecates Tholus, and Alba Patera, and one is on the rim of the Valles Marineris canyon system.

Implications: Given our age-dating results for valleys in the martian highlands, there are at least two possible interpretations consistent with our observations: (1) One interpretation is that the consistent age of all the valleys shown in Fig. 4 (which essentially overlap within error) imply they were active during a common, global formation period, and likely formed by a common mechanism, that then ended on a global scale. In this interpretation, the observed spread in Fig. 4 is observational or statistical and is not reflective of a major difference in age. (2) Alternatively, it is possible that the observed variability is a result of a real spread in the last activity in various valleys. In this case, valley formation may have been a sporadic, local process with more local sources. However, in either scenario, global scale, valley-forming activity on Mars occurred only during the first part of its history.

The few younger examples are concentrated in volcanic environments. One possible mechanism for forming these younger valleys is melting of surface ice or snow, driven by the enhanced heat flux in such a volcanic environments [14-16]. In this scenario, a confluence of two factors would be required to have formed 'young' valley systems on these volcanoes: availability of ice or snow on the surface and excess heat flux. If the confluence of these factors is rare, it might explain why valley networks are found on some relatively young (post mid-Hesperian) surfaces, but not on others.

Discussion: What do these results imply for models of valley network formation? A hypothesis that our results may help constrain is the idea that valley formation resulted from impact-driven climate change [17, 18]. Initially, models of this idea were focused on the climate effects of very large impactors, which would cause global-scale effects (a 100-km diameter impactor, which would form a ~ 500 -km diameter crater) [17]. More recently, examination of the effects of smaller impactors (such as a 6-km impactor, forming a ~ 60 km crater) have begun [18], and suggest that smaller impactors might trigger substantial-enough climate effects to cause precipitation and valley activity [18].

For these models to be consistent with our results, valley generation on regional-to-global scale has to largely end by the Early Hesperian. Although the cratering rate has decreased substantially since the mid-Hesperian, there still should have been ~ 200 craters 60-km or larger on Mars over this time period; in fact, there should have been a few 60-km-diameter craters formed on Mars over the last 100 Ma (integrating over the entire surface area of the planet) [9]. If craters of this scale were responsible for generating valleys early in the history of Mars, we might expect that these ~ 200 impacts since the mid-Hesperian would have led to precipitation and valley network activity that we could observe, which does not appear to be the case.

Our results do not rule out impact-generated climate changes as the responsible mechanism for the primary period of valley network formation, but it is a bit of a "Goldilocks" problem: if we assuming that other model conditions (such as a wet regolith) are met over much of martian history, there needs to be a significant chance of having one or more impacts of sufficient size to cause widespread valley activity as late as the Early Hesperian, but only a minimal chance that such an impact (or impacts) would occur and lead to widespread valley activity later than this point. The only way to meet these conditions is if the last extensive valley activity which we observe in the crater statistics was generated by only a small number of triggering events (one or a few). If this is the case, the intensity of the last impact-driven climate event (or events) must have been significant enough to cause large-scale re-integration of pre-existing valleys, or to widespread formation of new valley systems, so that valley could achieve a consistent Noachian/Hesperian age. We would suggest that the original focus on the rare 500-km diameter (or larger) crater-forming event (caused by a ~ 100 km diameter impactor) is a more promising avenue for exploration of this hypothesis than climate changes triggered by smaller impactors, which have occurred too frequently since the mid-Hesperian to be a major cause of valley activity on early Mars. A more complete understanding of the magnitude of climate change induced by very large impacts will be needed to test whether such a model is a viable mechanism for producing features consistent with what we observe on Mars.

References: [1] Carr, M.H. (1996) *Water on Mars*. [2] Craddock, R.A. and Howard, A.D. (2002) *JGR*, 107, 5111. [3] Gaidos, E. and Marion, G. (2003) *JGR*, 108, 5055. [4] Marsursky, H. et al. (1977) *JGR*, 82, 4016-4038. [5] Pieri, D.C. (1980) *Geomorphology of Martian valleys*, NASA TM-81979, 1-160. [6] Gulick, V.C. and Baker, V.R. (1990) *JGR*, 95, 14,325-14,244. [7] Mangold, N. et al. (2004) *Science*, 305, 78-81. [8] Scott, D.H. et al. (1995) USGS Misc. Invest. Ser., Map I-2461. [9] Neukum, G. and Ivanov, B.A. (2001) *LPSC XXXII*, 1757. [10] Hartmann, W.K. (2005) *Icarus* 174, 294-320. [11] McEwen, A.S et al. (2005) *Icarus*, 176, 351-381. [12] Namiki, N. and Solomon, S.C. (1994) *Science* 265, 929-933. [13] Melosh, H.J. (1989) *Impact Cratering: A Geologic Process*. [14] Gulick, V.C. (1997) *Icarus*, 130, 68-86. [15] Fassett, C.I. and Head, J.W. (2006) *Planet. Space Sci.*, 54, 370-378. [16] Fassett, C.I. and Head, J.W. (2007) *Icarus*, in press, doi: 10.1016/j.icarus.2006.12.021. [17] Segura, T.L. et al. (2002), *Science*, 298, 1977-1980. [18] Colaprete, A. et al. (2004), *2nd Conf. on Early Mars*, 8016.

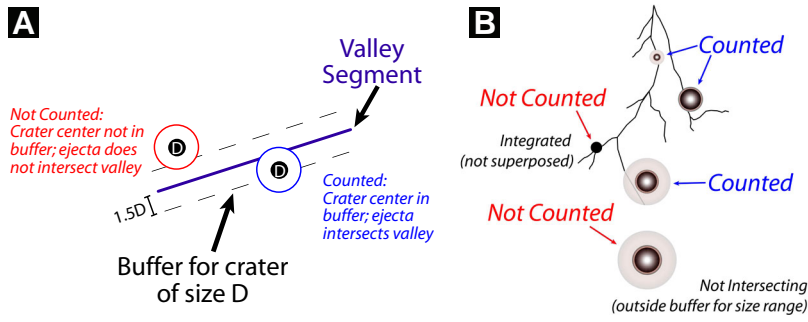


Figure 1. (A) A buffer is established for a given crater size, and craters are counted which 1) have their centers in the buffer and 2) intersect the valley segment. For each buffer, a count area is calculated (allowing for size-frequency determination). (B) A schematic of how this works for a variety of crater sizes. Craters that are not counted are either not superposed on the valley network (integrated), or outside the buffer appropriate for its crater size.

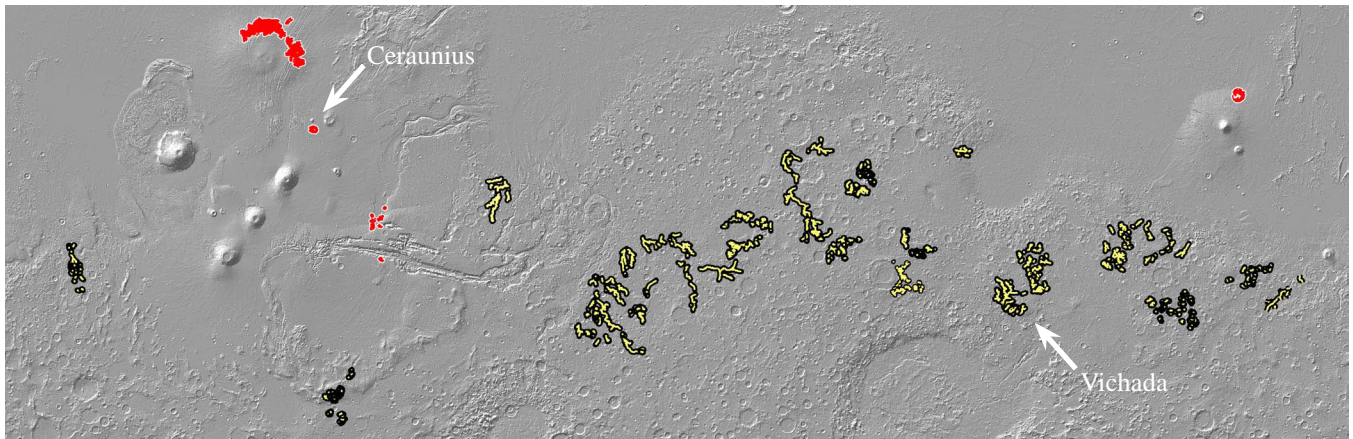


Figure 2. Locations of 30 valleys examined using the buffered count approach: features in yellow are Early Hesperian or older, and features in red have Late Hesperian or Early Amazonian ages (see Table 1, Fig. 4). Basemap is MOLA hillshade, 50 S to 50 N (Mercator).

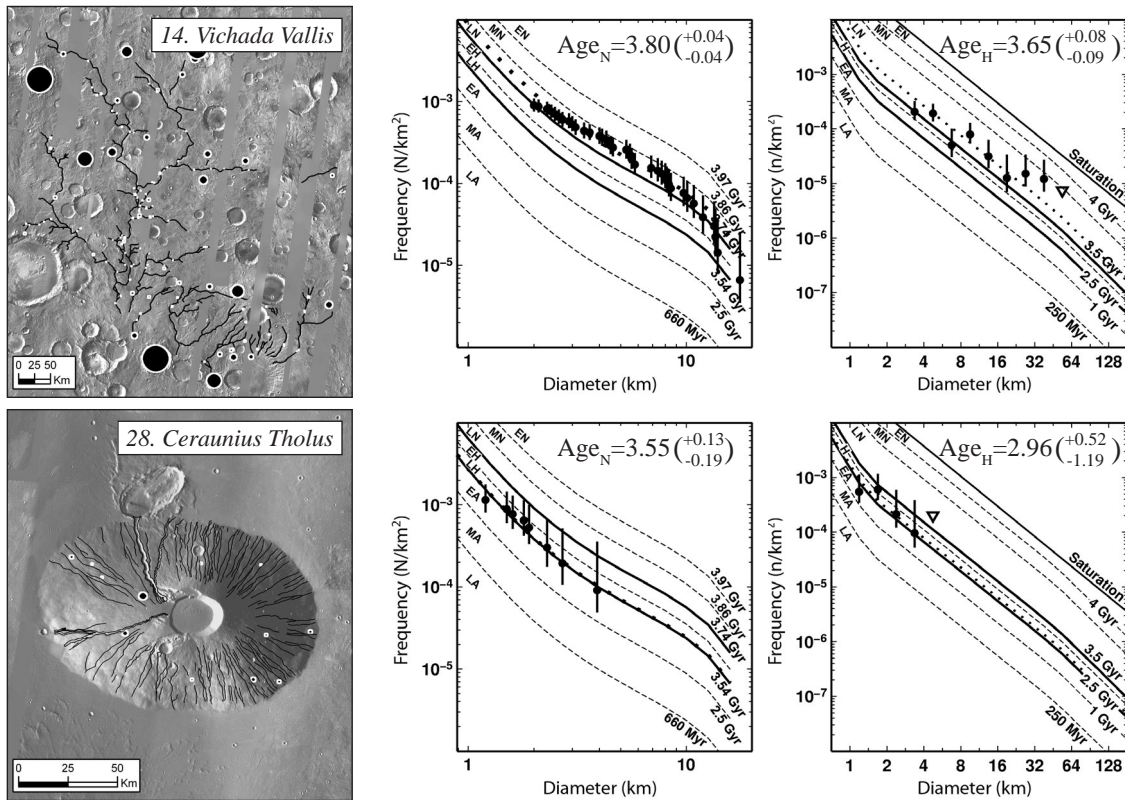


Figure 3. Example counts in two locations for Vichada Vallis and Ceraunius Tholus (see Fig. 2 for location). The center plots show a cumulative size-frequency distribution plot with isochrons using the Neukum production function [9], and the right plots show data as an incremental size-frequency distribution using Hartmann isochrons [10] (best fits are plotted as dots) Both approaches yield a Late Noachian age for Vichada and a Late Hesperian age for Ceraunius.

| # | Valley System | N(5) | Neuk. Age | Hart. Age | Neuk. Period | Hart. Period | # | Valley System | N(5) | Neuk. Age | Hart. Age | Neuk. Period | Hart. Period |
|----|--------------------|------|-----------|-----------|--------------|--------------|----|--------------------|------|-----------|-----------|--------------|--------------|
| 1 | Licus Vallis | 326 | 3.83 | 3.73 | LN | LN | 16 | Naktong and others | 160 | 3.7 | 3.5 | EH | LN/EH |
| 2 | 123E, 0N | 568 | 3.92 | 3.77 | MN | LN | 17 | 62.5E, -16N | 196 | 3.74 | 3.58 | EH | LN |
| 3 | 131E, -8N | 207 | 3.75 | 3.5 | LN | LN/EH | 18 | Tagus and others | 196 | 3.74 | 3.56 | EH | LN |
| 4 | 155E, -12.5N | 177 | 3.72 | 3.5 | EH | LN/EH | 19 | 132.5E, -22N | 160 | 3.7 | 3.45 | EH | EH |
| 5 | Al-Qahira Vallis | 416 | 3.87 | 3.71 | MN | LN | 20 | 96E, -11N | 207 | 3.75 | 3.54 | LN | LN/EH |
| 6 | Evros Vallis | 231 | 3.77 | 3.62 | LN | LN | 21 | Brazos and others | 160 | 3.7 | 3.46 | EH | EH |
| 7 | Meridiani: 0E, -5N | 168 | 3.71 | 3.54 | EH | LN | 22 | 65E, -9N | 290 | 3.81 | 3.62 | LN | LN |
| 8 | -9E, -5N | 290 | 3.81 | 3.67 | LN | LN | 23 | Cusus Vallis | 259 | 3.79 | 3.62 | LN | LN |
| 9 | 5E, -17N | 368 | 3.85 | 3.69 | LN | LN | 24 | -162E, -11N | 259 | 3.79 | 3.63 | LN | LN |
| 10 | Naro Vallis | 533 | 3.91 | 3.81 | MN | LN | 25 | Warrego Valles | 219 | 3.76 | 3.62 | LN | LN |
| 11 | Parana and others | 160 | 3.7 | 3.49 | EH | LN/EH | 26 | Nanedi and others | 231 | 3.77 | 3.59 | LN | LN |
| 12 | -13E, -7N | 244 | 3.78 | 3.61 | LN | LN | 27 | Hecates Tholus | 73 | 3.5 | 2.06 | EA | EA |
| 13 | -7E, -16N | 391 | 3.86 | 3.67 | MN | LN | 28 | Ceraunius Tholus | 85 | 3.55 | 2.96 | LH | LH |
| 14 | Vichada Vallis | 274 | 3.8 | 3.65 | LN | LN | 29 | VM/Echus Plateau | 48 | 3.28 | 1.98 | EA | EA |
| 15 | Nili: 77 E, 18 N | 308 | 3.82 | 3.74 | LN | LN | 30 | Alba Patera | 67 | 3.47 | 1.74 | EA | EA |

Table 1. Best fit age results for all valley counts; N(5) ages are calculated assuming the best-fit Neukum production function [9]. There are systematic differences in the Neukum and Hartmann age systems (ages in the Hartmann system are systematically younger), but there are only minimal differences in the geological period of last activity determined for a given valley.

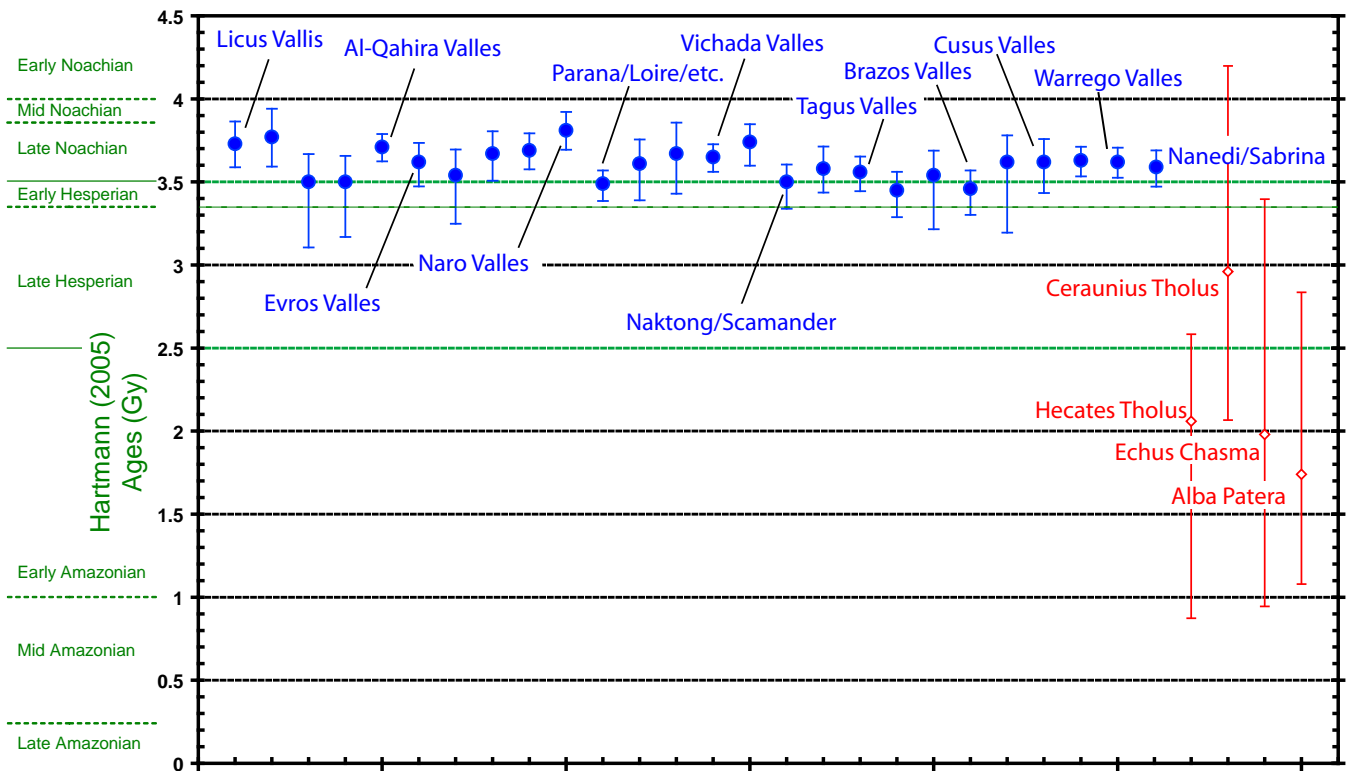


Figure 4. A summary of all ages determined for the valley systems in the Hartmann age system (see also Table 1). All ‘classic’ highland valley networks have ages in the Early Hesperian or earlier (most near the Noachian-Hesperian boundary). Error bars are 2-sigma and are a combination of two elements: (1) uncertainty of the fit for the best-fit isochron, and (2) Poisson counting statistics. The large error bars for the younger features is primarily a result of the downturn in the modelled cratering rate by the Hesperian: there is a greater difference in crater density between surfaces that are 3.7 Gyr old & 3.6 Gyr old than 3 Gyr & 2 Gyr in the model of the declining rate of cratering [see, e.g., 10]. Uncertainties shown here do not include the inherent uncertainty in the absolute calibration of the Martian age system or in the location of the period boundaries in the Hartmann system. Any change in the absolute calibration will have no effect on the relative age determinations and should not alter the main conclusions of this study.